Nucleic Acids Research, 2001, Vol. 29, No. 2 565–572

Unwinding of nucleic acids by HCV NS3 helicase is sensitive to the structure of the duplex

Alan J. Tackett, Lai Wei[1], Craig E. Cameron[1] and Kevin D. Raney*

Department of Biochemistry and Molecular Biology, University of Arkansas for Medical Sciences, Little Rock, AR 72205, USA and [1]Department of Biochemistry and Molecular Biology, Pennsylvania State University, University Park, PA 16803, USA

Received July 27, 2000; Revised and Accepted November 3, 2000

ABSTRACT

Hepatitis C virus (HCV) helicase, non-structural protein 3 (NS3), is proposed to aid in HCV genome replication and is considered a target for inhibition of HCV. In order to investigate the substrate requirements for nucleic acid unwinding by NS3, substrates were prepared by annealing a 30mer oligonucleotide to a 15mer. The resulting 15 bp duplex contained a single-stranded DNA overhang of 15 nt referred to as the bound strand. Other substrates were prepared in which the 15mer DNA was replaced by a strand of peptide nucleic acid (PNA). The PNA–DNA substrate was unwound by NS3, but the observed rate of strand separation was at least 25-fold slower than for the equivalent DNA–DNA substrate. Binding of NS3 to the PNA–DNA substrate was similar to the DNA–DNA substrate, due to the fact that NS3 initially binds to the single-stranded overhang, which was identical in each substrate. A PNA–RNA substrate was not unwound by NS3 under similar conditions. In contrast, morpholino–DNA and phosphorothioate–DNA substrates were utilized as efficiently by NS3 as DNA–DNA substrates. These results indicate that the PNA–DNA and PNA–RNA heteroduplexes adopt structures that are unfavorable for unwinding by NS3, suggesting that the unwinding activity of NS3 is sensitive to the structure of the duplex.

INTRODUCTION

Approximately 4% of the population world wide is infected by hepatitis C virus (HCV). HCV establishes a chronic infection of the liver that causes cirrhosis and can lead to the development of hepatocellular carcinoma (1). Current drug therapies for HCV infection often fail to resolve viral infection, therefore, new approaches for treating HCV infection are necessary. Virus multiplication is dependent upon a series of proteins expressed from the HCV genome, including multiple non-structural proteins that likely participate in genome transcription and replication (1). In particular, non-structural protein 3 (NS3) contains protease and helicase activities and is considered an important target for anti-HCV therapies.

Helicases are enzymes required for replication, recombination, repair, transport and other metabolic events involving DNA or RNA (reviewed in 2–5). These enzymes exhibit an ATPase activity that is stimulated upon binding to nucleic acid. Structural and biochemical studies have shed light on potential mechanisms for these enzymes, however, the manner in which the energy from ATP hydrolysis is transduced to produce mechanical work remains unclear. For many helicases a single-stranded nucleic acid overhang adjacent to the duplex region serves to load the enzyme onto the substrate, thus permitting the enzyme to initiate unwinding *in vitro*. Whether the loading strand is 5′ or 3′ to the duplex leads to classification of the enzymes as 5′→3′ or 3′→5′, respectively. Helicases have been organized into a number of superfamilies based upon sequence homology (6). Several common helicase motifs have been identified, suggesting that some mechanistic aspects may be shared among the different families. NS3 is a 3′→5′ helicase classified in superfamily 2.

The mechanism for DNA unwinding by helicases has been described in terms of an 'active' or 'passive' mechanism (2). In the active mechanism the helicase is believed to bind to each strand of the duplex followed by active separation of the two strands. In the passive mechanism the helicase sequesters a single-stranded nucleic acid that forms due to thermal fluctuations at a single-stranded/double-stranded nucleic acid junction. Translocation along single-stranded (ss)DNA with a strong directional bias is required for duplex unwinding via a passive mechanism. An 'active, rolling' mechanism has been suggested for the Rep helicase from *Escherichia coli* (7,8). Biochemical evidence for this functionally dimeric helicase has led to a model in which each subunit participates in binding and unwinding of double-stranded (ds)DNA. The two Rep subunits alternate positions at a single-stranded/double-stranded DNA junction in a process driven by binding and hydrolysis of ATP. An active mechanism for unwinding has been proposed for PcrA, a monomeric helicase, based upon crystal structures of PcrA bound to a single-stranded/double-stranded DNA junction in the presence of ADP or an ATP analog (9). The structures suggest that this enzyme interacts with the duplex region. Recent biochemical evidence indicates that these interactions disrupt the duplex in an ATP-dependent fashion (10).

A loading strand is required to initiate unwinding by NS3, but interactions between the enzyme and the displaced strand or duplex region of the substrate have not been well defined. NS3 has been proposed to function using a passive mechanism

*To whom correspondence should be addressed. Tel: +1 501 686 5244; Fax: +1 501 686 8169; Email: raneykevind@exchange.uams.edu

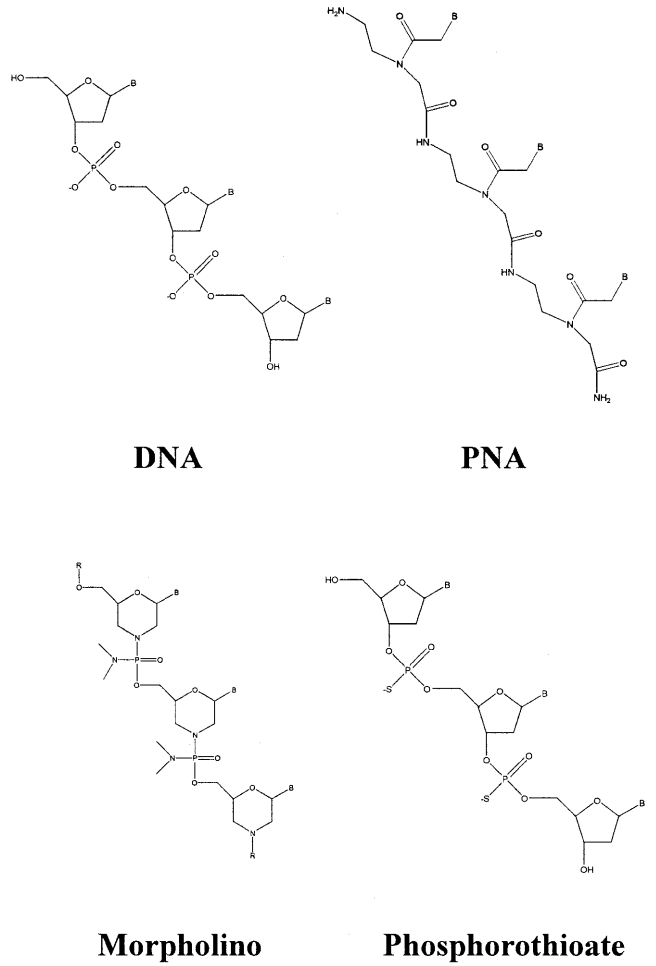

Figure 1. Structures of the DNA, PNA, morpholino and phosphorothioate oligonucleotides.

based upon kinetic measurements of duplex DNA unwinding (11). Additionally, NS3 separates blunt-ended, 5′-tailed and 3′-tailed duplex DNA in the absence of ATP (12). The crystal structure of the helicase domain bound to ssDNA led Kim *et al.* to suggest an inchworm model for unwinding that is consistent with a passive mechanism, however, the possibility of interactions between the helicase and the displaced strand was not eliminated (13). Others have investigated unwinding by NS3 using 2′-*O*-methyl RNA substrates and concluded that NS3 interacts only weakly with the displaced strand (14). Thus, evidence for a specific interaction between NS3 and the duplex region of the substrate is lacking.

We have investigated the substrate requirements for NS3 by replacing one of the duplex strands with an analog and measuring the effect of the modification on the kinetics of unwinding. Peptide nucleic acid (PNA)–DNA, PNA–RNA, morpholino–DNA and phosphorothioate–DNA substrates were evaluated (Fig. 1). We found that PNA–DNA and PNA–RNA heteroduplexes are poor substrates for unwinding by NS3 while DNA–morpholino and DNA–phosphorothioate duplexes serve as efficient substrates. These data provide evidence for an interaction between NS3 and the duplex region of substrates in addition to the loading strand.

MATERIALS AND METHODS

Materials

Phosphoenolpyruvate (tricyclohexylammonium salt), ATP (disodium salt), NADH, PMSF, pepstatin A, lysozyme, Sephadex G-25 and phosphoenolpyruvate kinase/lactate dehydrogenase (in glycerol) were obtained from Sigma. HEPES, EDTA, BME, SDS, MOPS, NaP, xylene cyanol, bromophenol blue, Tris, dextrose, IPTG, NaCl, ammonium sulfate, glycerol and $MgCl_2$ were obtained from Fisher. T4 polynucleotide kinase was purchased from New England Biolabs. NZCYM and Bacto-agar were obtained from Difco Laboratories. [γ-^{32}P]ATP was purchased from New England Nuclear. DNA oligonucleotides and phosphorothioate oligomers (Operon Technologies) and RNA oligonucleotides (Dharmacon Research) were purified by preparative polyacrylamide gel electrophoresis and stored in 10 mM HEPES pH 7.5, 1 mM EDTA as described (15). PNAs were prepared, purified and characterized as described (16). The morpholino oligomer was obtained from Gene Tools. Purified oligonucleotides were quantified by UV absorbance at 260 nm in 0.2 M KOH with calculated extinction coefficients. Macro-Prep High Q strong anion exchange support and Macro-Prep methyl HIC support were purchased from Bio-Rad Laboratories. Poly(U)–Sepharose 4B support and heparin–Sepharose CL-6B support were purchased from Pharmacia Biotech.

Cloning, expression and purification of NS3

The gene encoding HCV NS3 protease/helicase was amplified from an infectious HCV clone (genotype 1b) (17) by PCR as described previously (18). The following oligos were employed: NS3-helicase-for, 5′-GCGTCTAGACCGCGGT-GGA**GCGCCCATCACGGCCTACTCCCAAC**-3′; NS3-helicase-rev, 5′-GCGGAATTCAGATCT*TTACTA***AGTGAC-GACCTCCAGGTC**-3′. Sites used for cloning (*Sac*II in the for oligo and *Bgl*II in the rev oligo) are underlined and helicase coding sequences are shown in bold. Stop codons in the rev oligo are indicated by italics. The gene was cloned into the pET-ubiquitin vector system (18) using standard recombinant DNA methodology (19). The final construct was sequenced by the Pennsylvania State University Nucleic Acid Facility.

Escherichia coli BL21(DE3) cells were co-transformed with the plasmid encoding the NS3-ubiquitin fusion construct and a plasmid encoding the ubiquitin protease according to Novagen specifications. A 100 ml culture was grown overnight in NZCYM broth (pH 7.6) at 37°C. An aliquot of 5 ml of the overnight culture was used to inoculate a 500 ml culture in NZCYM broth (pH 7.6) at 37°C. The large scale culture was grown to an OD_{600} of 1.5. Dextrose (0.2%) and IPTG (0.5 mM) were added to the cultures and induction proceeded for 15 h at 15°C. Cells were harvested by centrifugation at 6500 *g* for 10 min in a Beckman JLA 10.500 rotor. Cell lysis was performed in purification buffer (25 mM Tris–HCl, pH 7.5, 1 mM EDTA, 5 mM BME, 10% glycerol) containing 0.5 M NaCl, 2 mM PMSF, 4 µg/ml pepstatin A and 0.2 mg/ml lysozyme. The lysate was passed through a nitrogen bomb, followed by sonication. The suspension was centrifuged at 48 000 *g* for 30 min in a Beckman JA 25.50 rotor. The supernatant was further clarified by centrifugation at 240 000 *g* for 2 h in a Beckman Type 50.2 Ti rotor. NS3 in the supernatant was purified by column chromatography following previous

Figure 2. Unwinding substrates utilized for NS3 assay. The strand containing the single-stranded overhang is defined as the loading strand and the complementary strand as the displaced strand. The substrates are labeled according to the strands of the duplex (D, DNA; R, RNA; P, PNA; S, phosphorothioate; M, morpholino). DD1 and DD2 differ only in the orientation of the duplex region, while DD3 and DD4 comprise totally different duplex regions. The base sequence of RR is identical to DD1.

procedures (20) with some modifications as described below. For all chromatographic steps fractions containing NS3 were identified by SDS–PAGE and ATPase assay. The supernatant was passed through a 30 ml Macro-Prep High Q strong anion exchange column equilibrated in purification buffer. NS3 does not bind to this column under these conditions. Protein was then precipitated by addition of ammonium sulfate to 55% saturation. After centrifugation the pellet was then suspended in purification buffer plus 0.5 M NaCl and 0.5 M ammonium sulfate. The suspension was then loaded onto a column containing 40 ml of Macro-Prep methyl HIC resin and eluted with a linear gradient of 1.5–0 M ammonium sulfate in purification buffer. Fractions containing NS3 were identified, collected and dialyzed against purification buffer plus 0.05 M NaCl. The dialyzed solution was loaded on a column containing 20 ml of poly(U)–Sepharose 4B and eluted with a linear gradient of 0.05–2 M NaCl in purification buffer. Fractions containing NS3 were dialyzed against purification buffer plus 0.05 M NaCl then loaded onto a column containing 30 ml of heparin–Sepharose CL-6B. NS3 was eluted by a linear gradient of 0.05–1 M NaCl in purification buffer. Appropriate fractions were collected, dialyzed against purification buffer plus 0.05 M NaCl, concentrated by ultrafiltration, frozen in liquid nitrogen and stored at –80°C. NS3 concentration was measured by UV absorbance at 280 nm using a calculated extinction coefficient of 64 000 M^{-1} cm^{-1}.

Helicase substrates

The sequences of the NS3 substrates are listed in Figure 2. Purified oligonucleotides were 5′-radiolabeled with T4 polynucleotide kinase at 37°C for 1 h. The kinase was inactivated by heating to 70°C for 10 min and unincorporated [γ-^{32}P]ATP was removed by passing the labeled oligonucleotides through two Sephadex G-25 spin columns. Helicase substrates were prepared by mixing equivalent amounts of radiolabeled oligonucleotide with the appropriate complementary strand, heating to 95°C for 10 min and then slow cooling.

NS3 unwinding assays

The NS3 unwinding substrate was a 30mer oligonucleotide (DNA or RNA) annealed to either a 15mer oligonucleotide (DNA or RNA), PNA, phosphorothioate or morpholino strand leaving a 3′-single-stranded overhang. Substrate (20 nM) was incubated for 10 min with 0.5 μM NS3 (unless otherwise stated) in 50 mM MOPS-K^+ pH 7.0, 50 μM EDTA at 25°C. Reactions with varying concentrations of NS3 were limited to a final concentration of 4 μM due to the stock concentration of purified NS3. The reaction was initiated by addition of 5 mM ATP, 4 mM phosphoenolpyruvate, phosphoenolpyruvate kinase/lactate dehydrogenase (10 and 15.5 U, respectively), 3.5 mM $MgCl_2$ and 250 nM 15mer trapping strand in 50 mM MOPS-K^+ pH 7.0. Reactions were quenched at various times by addition of 100 mM EDTA and 0.7% SDS. Aliquots from each time point were mixed with non-denaturing gel loading buffer (30% glycerol, 0.1% bromophenol blue, 0.1% xylene cyanol) and analyzed by electrophoresis on a 20% native polyacrylamide gel. The fractions of single-stranded 30mer and 30mer remaining in duplex form were determined with a Molecular Dynamics PhosphorImager and ImageQuant software. Data fitting was performed using the program Kaleidagraph (Synergy Software).

In order to measure the rate of strand separation for the RNA–RNA substrate and phosphorothioate–DNA substrate, unwinding assays were performed using a Kintek rapid chemical quench flow instrument at 25°C. The unwinding conditions were as described above. Rapid mixing of reactants was followed by varying incubation periods, after which the unwinding reaction was quenched with 100 mM EDTA and 0.7% SDS (21). The reaction products were analyzed as described above. Previous reports indicate that under conditions of excess enzyme over substrate NS3 can unwind duplexes in an ATP-independent fashion (12). Control experiments in the absence of ATP indicated that all unwinding reported here was dependent on the presence of ATP (data not shown).

Melting temperature analysis

The duplex portion of each substrate was used to determine the T_m value. These hybrids were prepared by heating a 1:1 mixture of oligonucleotides for 10 min at 95°C, then allowing the mixture to slowly cool. Substrates (4 μM) in 50 mM MOPS-K^+ pH 7.0, 2 mM NaCl, 50 μM EDTA were heated from 25 to 95°C at a rate of 0.7°C/min. The change in absorbance at 260 nm was observed on a Pharmacia Biotech spectrophotometer and the substrate melting temperature was determined using Swift software (Pharmacia Amersham).

Binding experiments

Binding experiments were performed using a Beacon fluorescence polarization system (PanVera). Substrates (0.5 nM) were composed of a 5′-fluorescein-labeled 30mer DNA annealed to

the appropriate 15mer as described above. Binding buffer consisted of 50 mM MOPS-K^+ pH 7.0, 50 μM EDTA. Titration with NS3 was followed by the change in polarization (mP). Binding data were fitted to a hyperbola using the program Kaleidagraph (Synergy Software).

RESULTS AND DISCUSSION

Rationale

An interaction between NS3 and the displaced strand of the duplex may occur with the sugar–phosphate backbone, possibly in a manner dependent upon electrostatic interactions (9,13). By changing the composition of the backbone of the displaced strand it is possible to evaluate the existence, nature and function of such an interaction. PNAs are polymers that mimic some of the properties of DNA (22). They are made up of the normal purine and pyrimidine bases linked together via a *N*-(2-aminoethyl)glycine backbone (Fig. 1). Bases of PNA pair with bases of DNA and RNA via formation of Watson–Crick hydrogen bonds. The heteroduplexes are often more stable than their DNA–DNA or RNA–RNA counterparts (23). The neutral, peptide-like structure of the PNA backbone would not be expected to participate in electrostatic interactions with NS3. The PNA backbone also lacks the steric bulk of the phosphodiester backbone, therefore, van der Waal's interactions between NS3 and the displaced strand of substrate might also change on using PNA.

Morpholino oligomers contain the nitrogenous bases that form Watson–Crick hydrogen bonds with complementary oligonucleotides (Fig. 1). A morpholino–DNA hybrid would maintain a neutral backbone while providing a larger interaction surface than PNA. In addition, these hybrids should have a thermal stability similar to that of a DNA–DNA substrate of equivalent sequence. Phosphorothioates are oligonucleotide analogs that contain a sulfur atom in place of an oxygen atom in the phosphate backbone (Fig. 1). This modification should only perturb interactions with NS3 if the size of the oxygen atom or length of the P-O bond is absolutely essential.

Substrate preparation

DNA, RNA, PNA, morpholino or phosphorothioate oligomers (15mers) were annealed to DNA or RNA oligonucleotides (30mers) to create the substrates shown in Figure 2. Substrates were named according to whether they contain DNA–DNA (DD), PNA–DNA (PD), RNA–RNA (RR), PNA–RNA (PR), phosphorothioate–DNA (SD) or morpholino–DNA (MD) duplexes. Two different sequences, DD1 and DD2, were designed in order to determine whether sequence modulates unwinding efficiency. Two additional substrates, DD3 and DD4, were designed to have different T_m values by altering the GC content relative to DD1 and DD2.

NS3 unwinding assays

To monitor helicase-catalyzed unwinding, conditions were employed in which enzyme concentration exceeded that of the substrate, as shown in Figure 3. NS3 was incubated with substrate and the reaction was initiated by addition of ATP. The 30mer is referred to as the 'loading strand' because it contains the single-stranded overhang necessary for optimal unwinding by NS3. In order to prevent spontaneous re-annealing of product strands, a trapping strand was introduced into the reaction mixture along with the ATP. Reactions were quenched by addition of EDTA (100 mM) and SDS (0.7%). Single-stranded reaction products were separated from duplex substrates by non-denaturing PAGE and visualized using a phosphorimager (Fig. 4). The PNA substrates were found to migrate more slowly than the unmodified substrates, presumably due to the lack of charge on the PNA strand (Fig. 4). To determine the amount of NS3 required for complete unwinding of the substrate, 20 nM DD1 was unwound with 0.25, 0.5 or 1 μM NS3 (Fig. 5A and Table 1). At each NS3 concentration employed substrate was unwound at similar rates. In the experiments described below a NS3 concentration of 0.5 μM was employed unless otherwise stated.

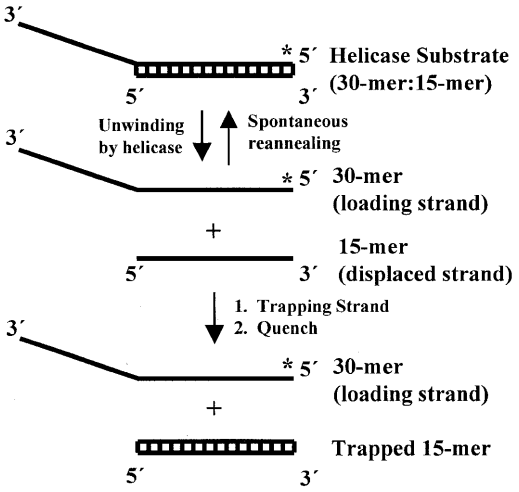

Figure 3. Assay for measuring helicase activity. Substrates are prepared by radiolabeling the loading strand and annealing the purified oligonucleotides. Helicase-catalyzed unwinding leads to production of a single-stranded nucleic acid that can re-anneal spontaneously. A trapping nucleic acid strand is included to prevent re-annealing, thereby allowing the products to be separated by gel electrophoresis.

Table 1. Unwinding rates for DD1, PD1 and RR at varying NS3 concentrations

NS3 (μM)	DD1[a], k (s^{-1})	PD1[a], k (s^{-1})	RR[b], k (s^{-1})
0.25	0.077 ± 0.001	–	–
0.5	0.077 ± 0.001	0.0010 ± 0.0003	0.25 ± 0.04
1	0.074 ± 0.001	0.0015 ± 0.0002	–
2	–	0.0024 ± 0.0002	0.27 ± 0.05
4	–	0.0034 ± 0.0001	–

[a]Rates were obtained by fitting data for unwinding to a single exponential using the program Kaleidagraph (Synergy Software). Errors are standard errors for the best fit of the data.
[b]Rates shown are for the first phase of the fit of the data to the sum of two exponentials.

PNA–DNA and PNA–RNA duplexes are poor substrates for unwinding by NS3

Substrates DD1 and DD2, which differ by inversion of the duplex region, were unwound with pseudo first order rate constants of

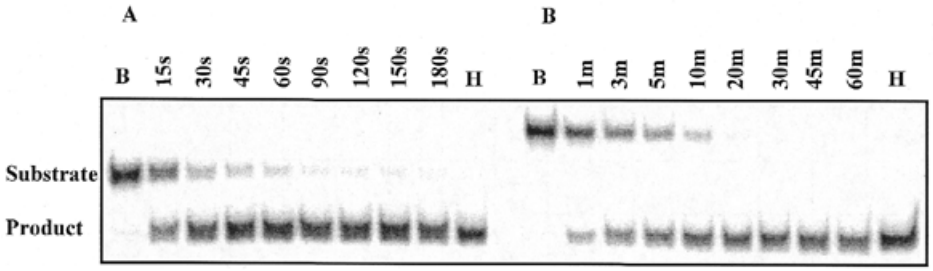

Figure 4. Separation of helicase-catalyzed reaction products by non-denaturing polyacrylamide gel electrophoresis. Unwinding by NS3 of the DD2 substrate (**A**) and the PD2 substrate (**B**). The blank (B) illustrates the unwinding substrate before the reaction is initiated, while the heated (H) sample shows trapping strand efficiency.

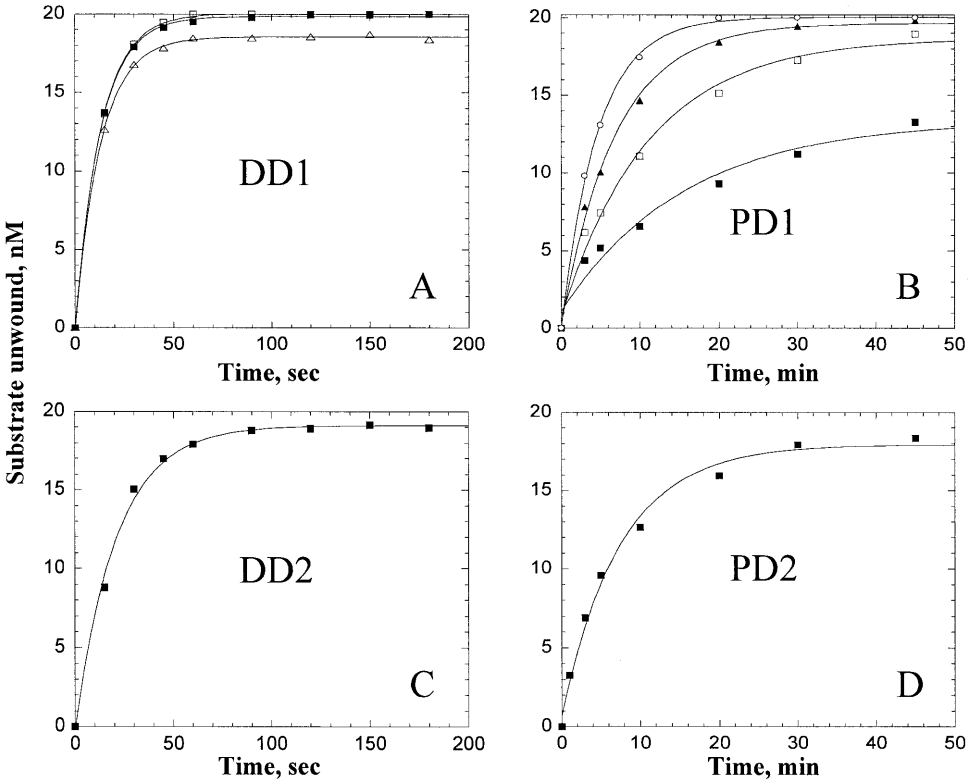

Figure 5. NS3-catalyzed unwinding of DNA–DNA and DNA–PNA substrates. Unwinding of DD1 (**A**) and the corresponding PD1 (**B**). Unwinding of DD2 (**C**) and the corresponding PD2 (**D**). Unwinding was performed at 0.25 (open triangles), 0.5 (filled squares), 1 (open squares), 2 (filled triangles) or 4 μM (open circles) NS3. Data were fitted to a single exponential using the program Kaleidagraph.

0.077 ± 0.001 and 0.047 ± 0.003 s^{-1}, respectively, suggesting minimal sequence dependence for unwinding of duplex DNA (Fig. 5A and C and Table 2). In contrast, the PNA–DNA substrates were unwound much slower (Fig. 5B and D). PD1 and PD2 were unwound with rate constants of 0.0010 ± 0.0003 and 0.0020 ± 0.0003 s^{-1}, respectively, which is 25- to 80-fold slower than the DNA–DNA substrates (Table 2). PD1 was not completely unwound at 0.5 μM, although increasing the concentration of NS3 up to 4 μM led to complete strand separation (Fig. 5B and Table 1). At 4 μM NS3 PD1 is unwound at a rate of 0.0034 ± 0.0001 s^{-1}, which is ~25-fold slower than DD1 (Table 1 and Fig. 6A). The increase in unwinding rates for the PNA–DNA substrate at increasing concentrations of NS3 indicates that NS3 binds poorly to PD1 or that slow unwinding leads to dissociation of NS3 prior to complete separation of the strands, so that multiple binding events are required for complete unwinding. To distinguish between these possibilities, equilibrium binding between NS3 and DD1 and PD1 was measured. A fluorescein-labeled 30mer was hybridized to either the 15mer DNA or 15mer PNA to prepare the substrates. NS3 was titrated into solutions containing 0.5 nM fluorescein-labeled DD1 or PD1 and fluorescence polarization was measured (Fig. 6B). The equilibrium binding constants were similar for each substrate. Therefore, NS3 binds to PD1 with similar

affinity to DD1, indicating that the difference in unwinding rates between these two substrates occurs due to slower unwinding of PD1, rather than weaker binding. The slow unwinding of PD1 is likely to lead to dissociation of NS3 from the substrate prior to complete separation of the duplex, which means that multiple association events are likely to occur on the time scale of the observed unwinding rate.

Table 2. Unwinding rates of substrates and melting temperatures of the duplex portion of each substrate[a]

Helicase substrate	Unwinding rate, k (s^{-1})	Melting temperature (°C)
DD1	0.077 ± 0.001	46.7
PD1	0.0010 ± 0.0003	71.1
SD	0.12 ± 0.02	38.7
DD2	0.047 ± 0.003	46.7
PD2	0.0020 ± 0.0003	77.5
MD	0.090 ± 0.004	57.2
DD3	0.089 ± 0.004	41.9
DD4	0.033 ± 0.001	55.3
RR[b]	0.25 ± 0.04	55.5
PR	–	74.3

[a]Unwinding was performed with 0.5 μM NS3. Rate constants were obtained by fitting the data to a single exponential using the program Kaleidagraph. Errors are standard errors from the best fit of the data. Melting temperatures were determined as described in Materials and Methods.
[b]Rate for the first phase from the best fit of the data to the sum of two exponentials.

The unwinding data for the RNA–RNA substrate best fitted the sum of two exponentials. The first exponential accounted for less than half of the substrate (8.9 nM) at a rate (0.25 ± 0.04 s^{-1}) that was slightly faster than the rate for unwinding of the DNA substrates (Fig. 7A and Table 1). The rate of the second phase was substantially slower (0.041 ± 0.019 s^{-1}). When the NS3 concentration was raised from 0.5 to 2 μM a larger fraction of RR was unwound in the first phase (12.3 nM), but the unwinding rates were similar (Fig. 7A and Table 1). Very little unwinding was observed for the PNA–RNA substrate (Fig. 7B), even when the concentration of NS3 was 2 μM (data not shown). Hence, the PNA–RNA duplex is poorly recognized by NS3. This result supports the notion that NS3 is sensitive to the structure of the duplex region.

Substrates with different thermal stabilities slightly alter NS3 unwinding efficiency

The melting temperatures of PNA–DNA and PNA–RNA heteroduplexes are higher than their corresponding unmodified duplexes. DD1 and DD2 had T_m values of 46.7°C whereas PD1 melted at 71.1°C and PD2 melted at 77.5°C (Table 2). The RNA–RNA duplex melted at 55.5°C and the PNA–RNA duplex melted at 74.3°C. Experiments were performed to determine if the increase in thermal stability of PNA–DNA substrates contributed to the slower unwinding rates. DNA–DNA substrates were prepared with varying GC contents and the T_m value of each substrate was measured (Table 2). DD3 had a T_m value of 41.9°C, which was 4.8°C lower than DD1, and DD4 had

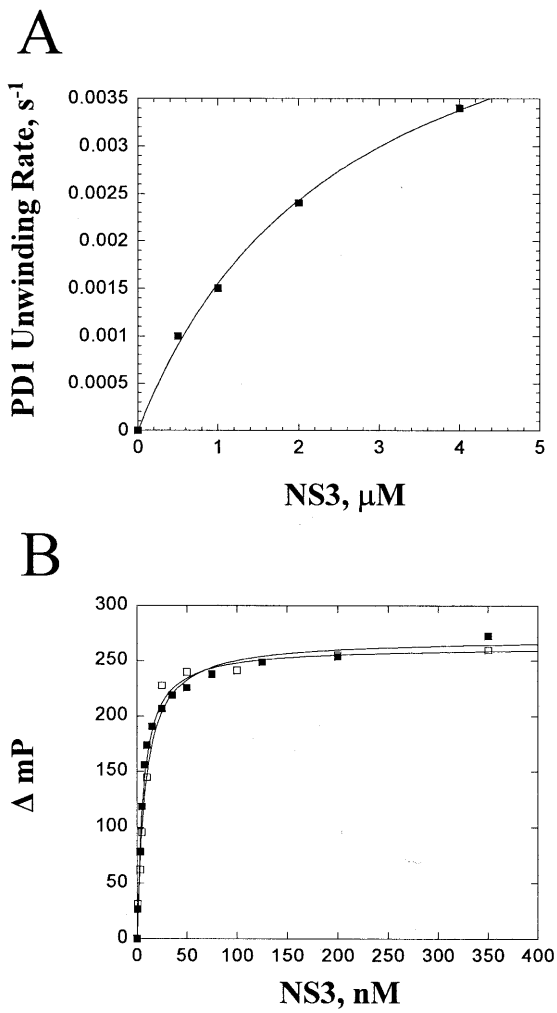

Figure 6. Unwinding of PD1 at varying NS3 concentration and binding of NS3 to DD1 and PD1. (**A**) The plot of PD1 unwinding rate as a function of NS3 concentration was fitted to a hyperbola. The fit produced an apparent K_d value of 2.5 ± 0.3 μM and a V_{max} of 0.0056 ± 0.0003 s^{-1}. (**B**) Equilibrium binding experiments were performed by titrating a solution containing 0.5 nM fluorescein-labeled DD1 (filled squares) or PD1 (open squares) with NS3. The fluorescence polarization was measured using a Beacon fluorescence polarization system (Pan Vera). Data were fitted to a hyperbola to obtain equilibrium binding constants. NS3 bound to DD1 and PD1 with K_d values of 6.3 ± 0.5 and 8.2 ± 0.8 nM, respectively.

a T_m value of 55.3°C, which was 8.6°C greater than DD1 (Table 2). The rate of unwinding of DD3 (0.089 ± 0.004 s^{-1}) was slightly faster than DD1, whereas the unwinding rate for DD4 (0.033 ± 0.001 s^{-1}) was somewhat slower than DD1 (Table 2). The observed trend is a decrease in the unwinding rate as the thermal stability of the substrate increases. However, changes in the T_m values of substrates are not sufficient to explain the dramatic reduction in unwinding efficiency observed for the PNA–DNA substrate (Table 2).

Morpholino–DNA and phosphorothioate–DNA substrates are unwound as efficiently as DNA–DNA substrates by NS3

A morpholino strand was used in place of the PNA strand and the rate of strand separation was measured. The unwinding rate

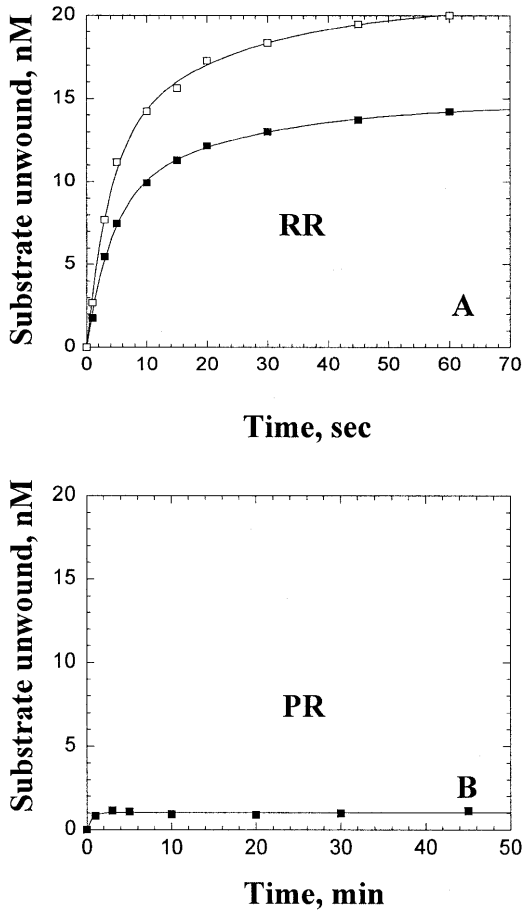

Figure 7. NS3-catalyzed unwinding of RNA substrates. Unwinding of RR (**A**) and the corresponding PR (**B**). Unwinding was performed with 0.5 (filled squares) and 2 μM (open squares) NS3. Data were fitted to the sum of two exponentials.

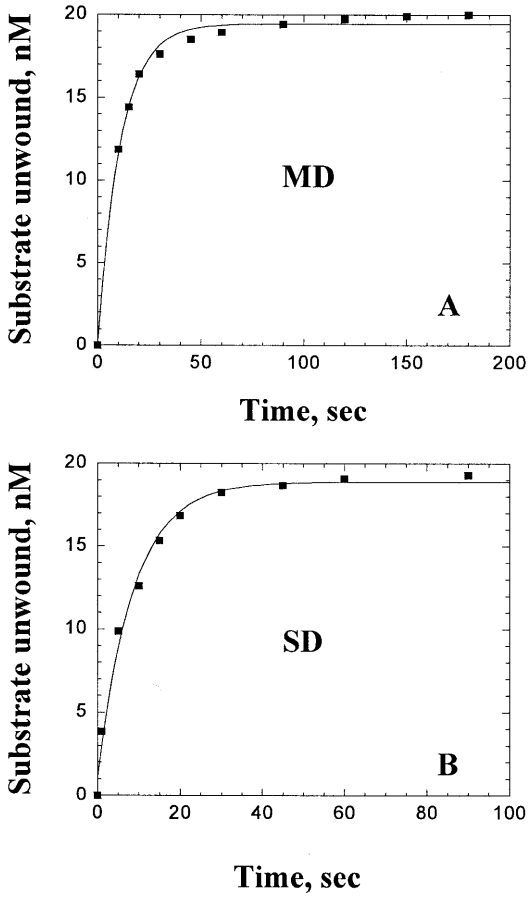

Figure 8. NS3-catalyzed unwinding of the morpholino–DNA substrate (**A**) and the phosphorothioate–DNA substrate (**B**). Unwinding was performed with 0.5 μM NS3. Data were fitted to a single exponential.

for morpholino–DNA was 0.090 ± 0.004 s^{-1}, which was slightly faster than the corresponding DNA substrate, DD2 (Fig. 8A and Table 2). The T_m value of morpholino–DNA was 57.2°C, which was similar to that of DD4 (Table 2). A phosphorothioate–DNA substrate was prepared and the rate of strand separation by NS3 was measured. The unwinding rate of phosphorothioate–DNA was 0.12 ± 0.02 s^{-1}, which was in close agreement with the rate for the corresponding DNA substrate, DD1 (Fig. 8B and Table 2). The T_m value of phosphorothioate–DNA was 38.7°C, which was somewhat lower than the DNA duplex (Table 2)

PNA–RNA duplexes adopt an A-like conformation (24), while PNA–DNA duplexes contain elements of B-form helices in many respects, except for base pair stacking, which is similar to A-form DNA (25). The number of base pairs per helical turn is 13 for PNA–DNA duplexes, as compared with 10 for B-form DNA. The interaction between helicases and nucleic acids has been proposed to rely upon electrostatic interactions with the deoxyribose phosphate backbone (9,13,26–28). PNA lacks the polyanion backbone of nucleic acids, thus PNA would not be expected to provide essential electrostatic interactions with a helicase.

At high NS3 concentration most of the RNA substrate was unwound in one phase at a slightly faster rate than the DNA substrates (Table 1). Therefore, NS3 does not strongly discriminate between A-form RNA and B-form DNA. However, when the displaced strand of the DNA and RNA substrates was replaced with a strand of PNA, the rate for unwinding was reduced by 25- to 80-fold for PNA–DNA substrates and little or no unwinding was observed with the PNA–RNA substrate (Table 2).

In contrast to PNA, exchange of the displaced strand of a substrate with either a morpholino or phosphorothioate strand did not result in reduced rates of unwinding (Fig. 8 and Table 2). PNA and morpholino oligomers both have a neutral backbone, while phosphorothioates have a charged backbone that resembles DNA (Fig. 1). Due to efficient unwinding of the morpholino substrate, the lack of a polyanion charge along the backbone does not account for the inhibition observed for PNA heteroduplexes. The structure of morpholino heteroduplexes has not been studied, but phosphorothioate–DNA duplexes have been shown to resemble a B-form helix with small differences in helical parameters (29). Thus, structural properties that appear to be unique to the PNA–DNA duplexes reduce the ability of NS3 to unwind these substrates. The remaining difference between the substrates is in the steric bulk of the

backbone. PNA has less steric bulk than morpholino and phosphorothioate oligos, suggesting that steric interactions between NS3 and the displaced strand may be responsible for optimal unwinding. The results with NS3 are in stark contrast to the bacteriophage T4 Dda helicase. Dda unwinds PNA–DNA substrates with similar rates to DNA–DNA substrates (21).

PNAs have been used to target various functions of DNA or RNA (22). PNAs have been used to inhibit enzymes such as DNA and RNA polymerases and ribosome progression when hybridized to DNA or RNA templates (30,31). One report has shown that a PNA capable of forming a triplex structure inhibited unwinding by the UL9 helicase (32). PNAs have also been used as probes to study substrate recognition by a nucleic acid binding enzyme. Interactions between the RNA component of telomerase with a DNA primer were identified using PNAs targeted to specific regions of the RNA (33). Recently, PNAs have been successfully introduced into cell cultures to inhibit telomerase by binding to its RNA component (34,35). Such an application might be useful to study replication of HCV in cell culture by targeting various regions of the RNA genome in order to interrupt RNA processing.

ACKNOWLEDGEMENTS

This investigation was supported by NIH grant AI47350 (K.D.R.), which includes a sub-contract to C.E.C. C.E.C. is the recipient of a Howard Temin Award (CA75118) from NCI, NIH.

REFERENCES

1. Nedderman,P., Tomei,L., Steinkuhler,C., Gallinari,P., Tramontano,A. and DeFrancesco,R. (1997) The nonstructural proteins of the hepatitis C virus: structure and functions. *Biol. Chem.*, **378**, 469–476.
2. Lohman,T.M. and Bjornson,K.P. (1996) Mechanisms of helicase-catalyzed DNA unwinding. *Annu. Rev. Biochem.*, **65**, 169–214.
3. Bird,L.E., Subramanya,H.S. and Wigley,D.B. (1998) Helicases: a unifying structural theme. *Curr. Opin. Struct. Biol.*, **8**, 14–18.
4. Egelman,E. (1996) Homomorphous hexameric helicases: tales from the ring cycle. *Curr. Biol.*, **4**, 759–762.
5. Matson,S.W., Bean,D.W. and George,J.W. (1994) DNA helicases: enzymes with essential roles in all aspects of DNA metabolism. *Bioessays*, **16**, 13–22.
6. Gorbalenya,A.E. and Koonin,E.V. (1993) Helicases: amino acid sequence comparisons and structure-function relationships. *Curr. Opin. Struct. Biol.*, **3**, 419–429.
7. Wong,I. and Lohman,T.M. (1992) Allosteric effects of nucleoside cofactors on *Escherichia coli* Rep helicase-DNA binding. *Science*, **256**, 350–355.
8. Amaratunga,M. and Lohman,T.M. (1993) *Escherichia coli* Rep helicase unwinds DNA by an active mechanism. *Biochemistry*, **32**, 6815–6820.
9. Velankar,S.S., Soultanas,P., Dillingham,M.S., Subramanya,H.S. and Wigley,D.B. (1999) Crystal structures of complexes of PcrA DNA helicase with a DNA substrate indicate an inchworm mechanism. *Cell*, **97**, 75–84.
10. Soultanas,P., Dillingham,M.S., Wiley,P., Webb,M.R. and Wigley,D.B. (2000) Uncoupling DNA translocation and helicase activity in PcrA: direct evidence for an active mechanism. *EMBO J.*, **19**, 3799–3810.
11. Porter,D.J.T. (1998) Product release is the major contributor to k_{cat} for the hepatitis C virus helicase-catalyzed strand separation of short duplex DNA. *J. Biol. Chem.*, **273**, 18906–18914.
12. Porter,D.J.T. and Preugschat,F. (2000) Strand-separating activity of hepatitis C virus helicase in the absence of ATP. *Biochemistry*, **39**, 5166–5173.
13. Kim,J.L., Morgenstern,K.A., Griffith,J.P., Dwyer,M.D., Thomson,J.A., Murcko,M.A., Lin,D. and Caron,P.R. (1998) Hepatitis C virus NS3 RNA helicase domain with a bound oligonucleotide: the crystal structure provides insights into the mode of unwinding. *Structure*, **6**, 89–100.
14. Hesson,T., Mannarino,A. and Cable,M. (2000) Probing the relationship between RNA-stimulated ATPase and helicase activities of HCV NS3 using 2′-*O*-methyl RNA substrates. *Biochemistry*, **39**, 2619–2625.
15. Raney,K.D. and Benkovic,S.J. (1995) Bacteriophage T4 Dda helicase translocates in a unidirectional fashion on single-stranded DNA. *J. Biol. Chem.*, **270**, 22236–22242.
16. Goodwin,T.E., Holland,R.D., Lay,J.O. and Raney,K.D. (1998) A simple procedure for solid-phase synthesis of peptide nucleic acids with N-terminal cysteine. *Bioorg. Med. Chem. Lett.*, **8**, 2231–2234.
17. Yanagi,M., St Claire,M., Shapiro,M., Emerson,S.U., Purcell,R.H. and Bukh,J. (1998) Transcripts of a chimeric cDNA clone of hepatitis C virus genotype 1b are infectious *in vivo*. *Virology*, **244**, 161–172.
18. Gohara,D.W., Ha,C.S., Ghosh,S.K.B., Arnold,J.J., Wisniewski,T.J. and Cameron,C.E. (1999) Production of "authentic" poliovirus RNA-dependent RNA polymerase (3D(pol)) by ubiquitin-protease-mediated cleavage in *Escherichia coli*. *Protein Expr. Purif.*, **17**, 128–138.
19. Sambrook,J., Fritsch,E.F. and Maniatis,T. (1989) *Molecular Cloning: A Laboratory Manual*, 2nd Edn. Cold Spring Harbor Laboratory Press, Cold Spring Harbor, NY.
20. Gallinari,P., Brennan,D., Nardi,C., Brunetti,M., Tomei,L., Steinkuhler,C. and De Francesco,R. (1998) Multiple enzymatic activities associated with recombinant NS3 protein of hepatitis C virus. *J. Virol.*, **72**, 6758–6769.
21. Raney,K.D., Hamilton,S. and Corey,D.R. (1998) In Nielsen,P.E. and Egholm,M. (eds), *Peptide Nucleic Acids*. Horizon Scientific Press, Wymondham, UK, pp. 241–251.
22. Nielsen,P.E. (1999) Peptide nucleic acids as therapeutic agents. *Curr. Opin. Struct. Biol.*, **9**, 353–357.
23. Egholm,M., Buchardt,O., Christensen,L., Behrens,C., Freier,S.M., Driver,D.A., Begg,R.H., Kim,S.K., Norden,B. and Nielsen,P.E. (1993) PNA hybridizes to complementary oligonucleotides obeying the Watson-Crick hydrogen-bonding rules. *Nature*, **365**, 566–568.
24. Brown,S.C., Thompson,S.A., Veal,J.M. and Davis,D.G. (1994) NMR solution structure of a peptide nucleic acid complexed with RNA. *Science*, **265**, 777–780.
25. Eriksson,M. and Nielsen,P.E. (1996) Solution structure of a peptide nucleic acid-DNA duplex. *Nature Struct. Biol.*, **3**, 410–413.
26. Yao,N., Hesson,T., Cable,M., Hong,Z., Kwong,A.D., Le,H.V. and Weber,P.C. (1997) Structure of the hepatitis C virus RNA helicase domain. *Nature Struct. Biol.*, **4**, 463–467.
27. Korolev,S., Hsieh,J., Gauss,G.H., Lohman,T.M. and Waksman,G. (1997) Major domain swiveling revealed by the crystal structures of complexes of *E. coli* Rep helicase bound to single-stranded DNA and ATP. *Cell*, **90**, 635–647.
28. SenGupta,D.J. and Boroweic,J.A. (1992) Strand-specific recognition of a synthetic DNA replication fork by the SV40 large tumor antigen. *Science*, **256**, 1656–1661.
29. Kanaori,K., Tamura,Y., Wada,T., Nishi,M., Kanehara,H., Morii,T., Tajima,K. and Makino,K. (1999) Structure and stability of the consecutive stereoregulated chiral phosphorothioate DNA duplex. *Biochemistry*, **38**, 16058–16066.
30. Hanvey,J.C., Peffer,N.C., Bisi,J.E., Thomsom,S.A., Cadilla,R., Josey,J.A., Ricca,D.J., Hassman,C.F., Bonham,M.A., Au,K.G. *et al.* (1992) Antisense and antigene properties of peptide nucleic acids. *Science*, **258**, 1481–1485.
31. Nielsen,P.E., Egholm,M. and Buchardt,O. (1994) Sequence specific transcription arrest by PNA bound to the template strand. *Gene*, **149**, 139–145.
32. Bastide,L., Boehmer,P.E., Villani,G. and Lebleu,B. (1999) Inhibition of DNA-helicase by peptide nucleic acids. *Nucleic Acids Res.*, **27**, 551–554.
33. Hamilton,S.E., Pitts,A.E., Katipally,R.R., Jia,S., Ruter,J.P., Davies,B.A., Shay,J.W., Wright,W.E. and Corey,D.R. (1997) Identification of determinants for inhibitor binding within the RNA active site of human telomerase. *Biochemistry*, **36**, 11873–11880.
34. Shammas,M.A., Simmons,C., Corey,D.R. and Reis,R.J.S. (1999) Telomerase inhibition by peptide nucleic acid reverses 'immortality' of transformed human cells. *Oncogene*, **18**, 6191–6200.
35. Hamilton,S.E., Simmons,C.G., Kathiriya,I.S. and Corey,D.R. (1999) Cellular delivery of peptide nucleic acids and inhibition of human telomerase. *Chem. Biol.*, **6**, 343–351.